SATELLITE DERIVED CLOUD PROPERTIES RELEVANT FOR CLOUD RADIATIVE FORCING: A CASE STUDY OF INTERACTION BETWEEN CLOUDS AND DUST AEROSOL PARTICLES

M. J. Costa [1, 2], E. Cattani [2], A. M. Silva [1], and V. Levizzani[2]

[1]Department of Physics and Évora Geophysics Centre, University of Évora, 7000 Évora, Portugal
[2]Institute of Atmospheric Sciences and Climate (ISAC-CNR), 40129 Bologna, Italy

1. INTRODUCTION

Clouds are the major factor regulating the Earth radiation budget. Special attention has been dedicated in the last few years to cloud interactions with aerosol particles through modeling studies, *in situ* measurements and remote sensing techniques (Bréon et al. 2002; Kawamoto and Nakajima 2003). Aerosols are considered responsible for significant modifications of cloud properties such as the decrease of the droplet size due to an increase in droplet concentration and respective enhancement of cloud reflectivity (Twomey 1974). In addition, changes in cloud lifetime and precipitation efficiency have also been suggested (Rosenfeld 1999, 2000). Particularly, aerosol particles mobilized in great quantities from desert areas, the “desert dust”, represent one of the main natural sources of atmospheric aerosol. Dust aerosol layers are capable of traveling thousands of kilometers at high altitudes, depending on the meteorological conditions. Apart from the possible consequences of cloud-aerosol interactions, desert dust particles apparently have a strong ability to act as ice nuclei. This statement is supported by observations of the conversion of supercooled water clouds to ice clouds at temperatures about 20ºC higher than those that are expected for homogeneous nucleation of cloud droplets in the middle and upper troposphere. This can lead to the formation of cirrus clouds at much higher temperatures than normally thought (Sassen 2002; DeMott et al. 2003).

The alterations suffered by clouds through their interaction with aerosols, specifically with desert dust, may have strong implications on the interaction with solar and terrestrial radiation, leading to different radiative forcing estimates with respect to clouds in “clean” atmospheric environments (continental or marine). The aim of the present work is to determine the cloud optical thickness (COT) and droplet effective radius (DER) (indicative properties of the possible cloud-aerosol interaction effect) of continental and marine cloud layers, which experience interaction with dust aerosol layers. These cloud properties are derived from the inversion of satellite spectral measurements in the visible (VIS) and near infrared (NIR) spectral regions (Nakajima and Nakajima 1995). The retrieved cloud properties are in turn used in combination with a suitable radiative transfer model to estimate the radiation fluxes and subsequently evaluate the cloud radiative forcing during selected episodes of strong desert dust transports. The methodology is applied to a summer 2002 case over southwestern Europe, during the VELETA 2002 (eValuation of the Effects of eLevation and aErosols on the ultravioleT rAdiation) intensive measurement campaign.

Corresponding author’s address: Maria João Costa, Department of Physics, University of Évora, Portugal; E-Mail: mjcosta@uevora.pt

2. METHOD

Satellite measurements are those of the MODerate Resolution Imaging Spectroradiometer (MODIS) onboard Terra and Aqua satellites (1 x 1 km^2 spatial resolution) in three spectral channels: 0.62 - 0.67 μm; 3.66 - 3.84 μm; 10.78 - 11.28 μm.

The methodology used to derived the cloud properties (Costa et al. 2004) consists of a first cloud detection phase and a subsequent step of particle phase determination (liquid water or ice), assuming that clouds at one time are made of either liquid water or ice particles (no mixed phase clouds are considered). The procedure relies on a bi-spectral technique that uses satellite measurements in the VIS and infrared (IR) spectral regions centered at 0.65 μm and 11 μm, respectively. The satellite measurements are initially classified in terms of the underlying surface (land or water) using a land-sea mask. Subsequently, the histograms of the VIS radiances and IR brightness temperatures are analyzed to determine threshold values that define the limits between clear sky, water clouds and ice clouds. Such threshold classification is done at the pixel level and when the pixel is cloudy, four possible cases are distinguished: water clouds over the ocean, ice clouds over the ocean, water clouds over land, and ice clouds over land.

The VIS, NIR (centered at 3.75 μm) and IR radiance measurements corresponding to the pixels classified in the four categories are used to retrieve cloud optical thickness, effective radius and cloud top temperature using the algorithm proposed by Nakajima and Nakajima (1995) and Kawamoto et al. (2001). The four categories are treated separately because relevant differences in cloud and surface characterization must be taken into account. The algorithm relies on the comparison between the modeled cloud radiances in the three spectral bands and the corresponding satellite radiance measurements. The latter are deprived of the undesirable components, such as the solar radiation reflected by the surface and the thermal radiation emitted from the cloud layer and the surface, in order to retain only the cloud signal. These corrections are based on the use of LookUp Tables (LUTs) calculated using the radiative transfer code RSTAR (Nakajima and Tanaka 1986, 1988). The LUTs contain the radiative quantities necessary for the cloud properties retrieval, namely the cloud reflected radiances and hemispherical albedo in the VIS and NIR, the transmission in the VIS, NIR and IR spectral bands and the reflection and atmospheric emitted radiation in the NIR and IR spectral bands. The LUTs are built for a grid of selected values of the COT, DER, cloud top temperature, equivalent water vapor above the cloud, equivalent water vapor of the cloud layer, solar zenith, satellite zenith and relative azimuth angles. The cloud is characterized by a lognormal hydrometeor size distribution. Mean values of surface temperature and reflectance, as well as a mid latitude summer atmospheric vertical profile (McClatchey et al. 1971), are used. Besides the cloud optical thickness, effective radius, and top temperature, the cloud top height and pressure are also retrieved from the top temperature values by linear interpolation of the selected atmospheric vertical profile.

3. RESULTS

The case study refers to the period 15 - 20 July 2002 during the VELETA 2002 intensive field campaign in the south of the Iberian Peninsula (Sierra Nevada area, Spain; see Fig. 1). Measurements from a set of radiometers and sun/sky photometers installed in several locations in the area, as well as LIDAR measurements (Alados-Arboledas et al. 2003) were available along with other data. The first days of the case study were characterized by extremely clear conditions in terms of the atmospheric aerosol load (background situation). In the last days of the campaign (18 - 20 July 2002) a dust plume coming from North Africa (Sahara) overpassed the area and was detected by the LIDAR at the same atmospheric level as the cloud systems.

3.1 Cloud Properties

The analysis was initially concentrated on the retrieved effective radius values to detect any cloud modification induced by the aerosol. The particle effective radius for each day was averaged in the area delimited by the dashed box 1 in Fig. 1.

In the first two days (15 and 16 July) there were very few clouds (mainly stratiform) forming over the Mediterranean Sea in the area of box 1. On 17 July, one day prior the start of the dust transport event over the area, most of the clouds were developing over land; the averaged effective radius and the respective standard deviation are 7.9 ± 1.3 μm. In this case, the cloud top height was of about 1km. Two days later (19 July) the averaged effective radius and standard deviation are 6.2 ± 1.2 μm. Clearly there was a decrease of the mean particle effective radius in the area, which may be an indication that clouds were subject to the influence of dust aerosol particles. Additional information from the LIDAR measurements in the area of Granada (see square in box 1 of Fig. 1) indicate that the dust aerosol layer extended approximately from 2 to 4 km height. The cloud top height for the same day over the area is shown in the frequency histogram of Fig. 2. More than 60% of the cloudy pixels in the area are associated to cloud top height values between 2 and 4 km, which hints to the dust aerosol particles detected by the LIDAR system at the same level being incorporated by the clouds developing in the area. Moreover, this fact supports the hypothesis that the calculated effective radius

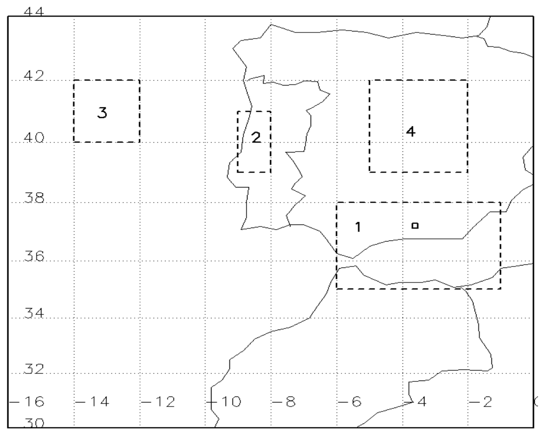

Figure 1. Map of the geographical area considered in the study. The dashed boxes indicate the areas selected for the analysis of the: 1) particle effective radius variation; 2) clouds in dust free atmosphere; 3) maritime clouds in dusty atmosphere; 4) continental clouds in dusty atmosphere. The square inside box 1 indicates the location where the VELETA field campaign took place. Boxes 2, 3, and 4 correspond to different days.

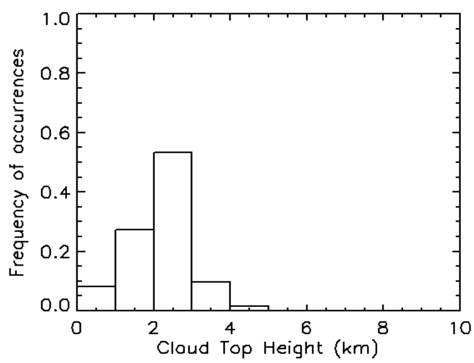

Figure 2. Frequency histogram of cloud top height derived for 19 July 2002, 1340 UTC, over the area delimited by the dashed box 1 in Fig. 1.

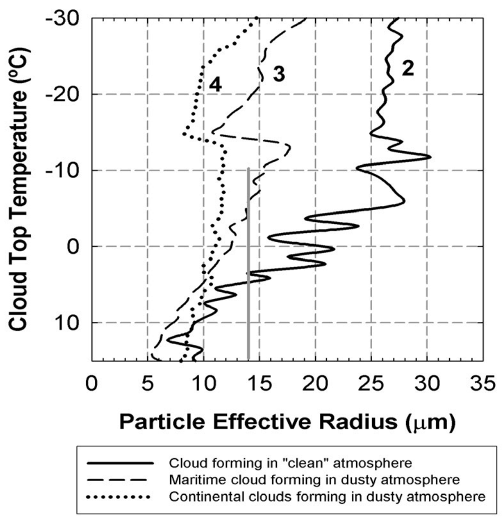

Figure 3. Cloud top temperature as a function of particle effective radius derived for three different situations. The numbers indicate the correspondence with the dashed boxes of Fig. 1. The vertical gray line indicates the 14 μm precipitation threshold (Rosenfeld and Gutman 1994).

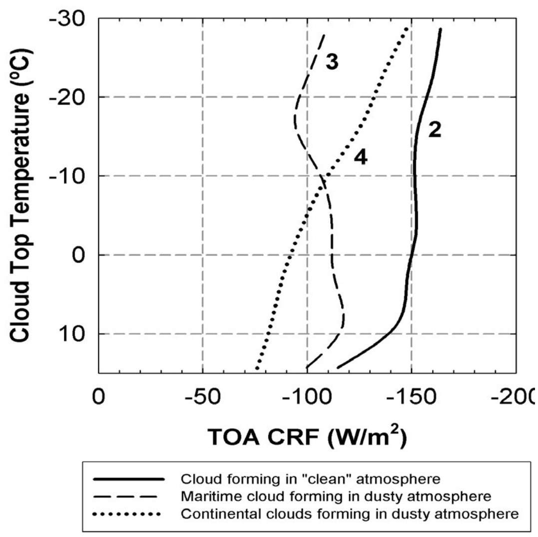

Figure 4. Cloud radiative forcing at the top of the atmosphere for the curves in Fig. 3.

decrease (7.9 μm on 17 to 6.2 μm on 19 July) is due to the interaction of clouds with dust aerosol particles.

The relation between the effective radius and the cloud top temperature for developing convective clouds can reveal information on the microphysical processes occurring in the cloud, and consequently on the precipitation formation process (Rosenfeld and Lensky 1998). The evolution of the particle effective radius as the cloud top temperature decreases is investigated in Fig. 3 for three selected situations: clouds forming in a dust-free atmosphere; clouds over a maritime environment forming in the presence of dust particles; clouds forming in a continental dusty atmosphere. Each curve represents the median effective radius value for each 1ºC temperature interval, corresponding to the dashed boxes in Fig. 1. The vertical solid gray line in Fig. 3 represents the 14 μm precipitation threshold beyond which precipitation from convective clouds is likely to occur (Rosenfeld and Gutman 1994). Box 2 in Fig. 1 (curve 2 in Fig. 3) delimits an area where convective clouds were developing out of a clean maritime atmosphere. The evolution of the particle radius in this case allows for distinguishing the microphysical zones defined by Rosenfeld and Lensky (1998): in the lower atmosphere cloud droplet size increases probably by coalescence, followed by a rainout zone between 20 and 25 μm. As the cloud top temperature decreases, a mixed phase can be distinguished followed by the glaciated zone, which is reached at a temperature of about -15ºC. Curve 3 in Fig. 3 (box 3 in Fig. 1) represents the effective radius evolution for maritime clouds growing in presence of dust particles. As for curve 4 (box 4 in Fig. 1), it represents the evolution of a continental cloud developing also in presence of dust. In both cases, the microphysical zones distinguished for curve 2 are not present and a zone extending down to below –10ºC in the case of continental clouds (curve 4) shows up where cloud droplets grow apparently by diffusional growth (slower growth than by coalescence). Maritime dusty clouds (curve 3) reach the 14 μm precipitation threshold but it is not clear if the rainout process actually occurs. Both cases seem to present a mixed phase that extends from –15ºC to lower temperature values.

3.2 Direct Cloud Radiative Forcing

The cloud radiative forcing (CRF) was calculated from the net shortwave (N_{SW}) and longwave (N_{LW}) fluxes at the top of the atmosphere (TOA) according to equation 1, being the net fluxes given by N_{SW} =*SW*↓-*SW*↑ and N_{LW} =*LW*↓-*LW*↑).

$$CRF = (N_{SW} + N_{LW})^{cloud} - (N_{SW} + N_{LW})^{\mathrm{clear}} \qquad (1)$$

The fluxes are calculated with the RSTAR code (Nakajima and Tanaka 1986, 1988), using the derived cloud properties. The graph in Fig. 4 shows the cloud radiative forcing derived for the situations in Fig. 3. Note that the cloud developing in the dust-free atmosphere (curve 2) presents the most negative forcing, slightly increasing as the temperature decreases. As for the continental cloud growing in the presence of dust (curve 4), it presents the lowest (less negative) TOA CRF values at temperatures above –10ºC, becoming increasingly higher towards the highest atmospheric layers, even higher than that obtained for the maritime clouds contaminated with dust.

4. CONCLUSIONS

The case studied revealed a decrease of the cloud droplet effective radius when dust aerosol particles were present over the area and at the same atmospheric levels. The evolution of the cloud top temperature and the effective radius for convective clouds in the area indicates that clouds that come in contact with dust particles are in fact affected by them: particles grow less and this most probably affects precipitation, diminishing or even suppressing it. The corresponding TOA CRF was subsequently calculated and found that the “clean” clouds reflect more radiation to space than the dust contaminated ones.

5. ACKNOWLEDGEMENTS

MODIS data were acquired as part of the NASA's Earth Science Enterprise. The algorithms were developed by the MODIS Science Teams. The data were processed by the MODIS Adaptive Processing System (MODAPS) and Goddard Distributed Active Archive Center (DAAC), which also archives and distributes them. The authors are grateful to the OpenCLASTR project (http://www.ccsr.u-tokyo.ac.jp/~clastr/) for making available the RSTAR (system for transfer of atmospheric radiation) and CAPCOM (Comprehensive Analysis Program for Cloud Optical Measurement) packages for use in this research. This study was funded by EURAINSAT (http://www.isac.cnr.it/~eurainsat/), a shared-cost project (contract EVG1-2000-00030) co-funded by the Research Directorate General of the European Commission within the research and technological development activities of a generic nature of the Environment and Sustainable Development subprogram (5th Framework Programme). Funding was also provided by the Portuguese Foundation for Science & Technology under grant POCTI/CTA/42917/2001. We thank the MADOC, the Armilla Air Force Base, The Sierra Nevada National Park and the City Halls of Pitres and Motril, Granada, Spain, for their gracious support. The authors also thank José António Rodrigues for providing the LIDAR measurements.

One of the authors (MJC) was financially supported by the Subprograma Ciência e Tecnologia do 2º Quadro Comunitário de Apoio.

6. REFERENCES

Alados-Arboledas, L., J. Lorente J. A. Martínez, V. Cachorro, A. Labajo, B. De la Morena, J. P. Díaz, M. Pujadas, H. Horvath, A. M. Silva, G. Pavesse, and J. Rodrigues, 2003: VELETA 2002 field campaign. *Geophys. Res. Abstracts*, **5**, 12218.

Bréon, F.-M., D. Tanré, and S. Generoso, 2002: Aerosol effect on cloud droplet size monitored from satellite. *Science*, **295**, pp 834-838.

Costa, M. J., E. Cattani, V. Levizzani, and A. M. Silva, 2004: Cloud microphysical properties retrieval during intense biomass burning events over Africa and Portugal. In: *Measuring precipitation from space: EURAINSAT and the future*, V. Levizzani, P. Bauer, and F. J. Turk Eds., Kluwer Acad. Publ., Dordrecht (The Netherlands), *submitted*.

DeMott, P. J., K. Sassen, M. Poellot, D. Baumgardner, D. C. Rogers, S. Brooks, A. J. Prenni, and S. M. Kreidenweis, 2003: African dust aerosols as atmospheric ice nuclei. *Geophys. Res. Lett.*, **30**, No. 14, 1732, doi:10.1029/2003GL017410.

Kawamoto, K., T. Nakajima, and T. Y. Nakajima, 2001: A global determination of cloud microphysics with AVHRR remote sensing. *J. Climate*, **14**, 2054-2068.

Kawamoto, K., and T. Nakajima, 2003: Seasonal variation of cloud particle size from AVHRR remote sensing. *Geophys. Res. Lett.*, **30**, 1810-1813.

McClatchey, R. A., W. Fenn, J. E. A. Selby, F. E. Volz, and J. S. Garing, 1971: Optical properties of the Atmosphere. AFCRL-TR- 71-0279, *Envir. Research Papers*, **354**, Air Force Cambridge Research Laboratories, Hanscom AFB, Bedford, MA, 85 pp.

Nakajima, T. Y., and T. Nakajima, 1995: Wide-area determination of cloud microphysical properties from NOAA AVHRR measurements for FIRE and ASTEX regions. *J. Atmos. Sci.*, **52**, 4043-4059.

Nakajima, T., and M. Tanaka, 1986: Matrix formulation for the transfer of solar radiation in a plane-parallel scattering atmosphere. *J. Quant. Spectrosc. Radiat. Transfer*, **35**, 13-21.

Nakajima, T., and M. Tanaka, 1988: Algorithms for radiative intensity calculations in moderately thick atmospheres using a truncation approximation. *J. Quant. Spectrosc. Radiat. Transfer* , **40**, 51-69.

Rosenfeld, D., and G. Gutman, 1994: Retrieving microphysical properties near the tops of potential rain clouds by multispectral analysis of AVHRR data. *Atmos. Res.*, **34**, 259-283.

Rosenfeld, D., and I. Lensky, 1998: Satellite-based insights into precipitation formation processes in continental and maritime convective clouds. *Bull. Amer. Meteor. Soc.*, **79**, 2457-2476.

Rosenfeld, D., 1999: TRMM observed first direct evidence of smoke from forest fires inhibiting rainfall. *Geophys. Res. Lett.*, **26**, 3105-3108.

Rosenfeld, D., 2000: Suppression of rain and snow by urban and industrial air pollution. *Science*, **287**, 1793-1796.

Sassen, K., 2002: Indirect climate forcing over the western US from Asian dust storms. *Geophys. Res. Lett.*, doi:10.1029/2001GL014034.

Twomey, S., 1974: Pollution and the planetary albedo. *Atmos. Res.*, **8**, 1251-1256.